Received: 6 August 2020 | Revised: 24 December 2022 | Accepted: 25 December 2022

DOI: 10.1111/aje.13114

African Journal of Ecology WILEY

RESEARCH ARTICLE

Integrating RADAR and optical imagery improve the modelling of carbon stocks in a mopane-dominated African savannah dry forest

Tawanda W. Gara[1] | Kudzai S. Mpakairi[2] | Tinotenda C. Nampira[3] | Joseph Oduro Appiah[4] | Tasiyiwa P. Muumbe[5] | Timothy Dube[2]

[1]Department of Environmental Science and Management, California State Polytechnic University Humboldt, Arcata, California, USA

[2]Department of Earth Sciences, Institute of Water Studies, University of the Western Cape, Bellville, South Africa

[3]Department of Geography, Geospatial Sciences and Earth Observation, University of Zimbabwe, Harare, Zimbabwe

[4]Department of Geography, Environment and Spatial Analysis, California State Polytechnic University Humboldt, Arcata, California, USA

[5]Department for Earth Observation, Friedrich Schiller University Jena, Jena, Germany

Correspondence
Tawanda W. Gara, Department of Environmental Science and Management, California State Polytechnic University Humboldt, Arcata 95521, CA, USA.
Email: tw4gara@gmail.com and tawanda.gara@humboldt.edu

Abstract

This study examined the integration of two satellite data sets, that is Landsat 7 ETM+ and ALOS PALSAR (Advanced Land Observing Satellite Phased Array type L-band Synthetic Aperture RADAR) in estimating carbon stocks in mopane woodlands of north-western Zimbabwe. Mopane woodlands cover large spatial extents and provide ecosystem benefits to the rural economies and grazing resources for both livestock and wildlife. In this study, artificial neural networks (ANN) were used to estimate carbon stocks based on spectral metrics derived from Landsat 7 ETM+ and ALOS PALSAR. To determine the utility of the two satellite-derived metrics, a two-pronged modelling framework was adopted. Firstly, we used spectral bands and vegetation indices from the two satellite data sets independently, and subsequently, we integrated the metrics from the two satellite data sets into the final model. Results showed that the ALOS PALSAR (R^2 = 0.75 and nRMSE = 0.16) and Landsat ETM+ (R^2 = 0.78 and nRMSE = 0.14) derived spectral bands and vegetation indices comparatively yielded accurate estimations of carbon stocks. Integrating spectral bands and vegetation indices from both sensors significantly improved the estimation of carbon stocks (R^2 = 0.84 and nRMSE = 0.12). These findings underscore the importance of integrating satellite data in vegetation biophysical assessment and monitoring in poorly documented ecosystems such as the mopane woodlands.

KEYWORDS
ALOS PALSAR, carbon monitoring, climate change, Landsat 7 ETM+, sensor integration

Résumé

Cette étude a examiné l'intégration de deux ensembles de données satellitaires, notamment Landsat 7 ETM+ et ALOS PALSAR (Advanced Land Observing Satellite Phased Array type L-band Synthetic Aperture RADAR) dans l'estimation des stocks de carbone dans les forêts de Mopane au nord-ouest du Zimbabwe. Les forêts de Mopane couvrent de vastes étendues d'espace et offrent des avantages écosystémiques aux économies rurales et des ressources de pâturage pour le bétail et la faune. Dans cette étude, des réseaux de neurones artificiels (ANN) ont été utilisés pour estimer les stocks de carbone sur la base d'indicateurs spectraux dérivés de Landsat 7 ETM+ et

ALOS PALSAR. Pour déterminer l'utilité des deux indicateurs dérivés des satellites, un cadre de modélisation à deux volets a été adopté. Premièrement, nous avons utilisé indépendamment les bandes spectrales et les indices de végétation des deux ensembles de données satellitaires, puis nous avons intégré les indicateurs des deux ensembles de données satellitaires dans le modèle final. Les résultats ont montré que les bandes spectrales dérivées et les indices de végétation d'ALOS PALSAR (R^2 = 0,75 et nRMSE = 0,16) et Landsat ETM+ (R^2 = 0,78 et nRMSE = 0,14) ont comparativement donné des estimations précises des stocks de carbone. L'intégration des bandes spectrales et des indices de végétation des deux capteurs a considérablement amélioré l'estimation des stocks de carbone (R^2 = 0,84 et nRMSE = 0,12). Ces résultats mettent en évidence l'importance de l'intégration des données satellitaires dans l'évaluation et la surveillance biophysiques de la végétation dans les écosystèmes mal documentés comme les forêts de Mopane.

1 | INTRODUCTION

Forests are key environments and provide an important pathway in reducing the effects of climate change. They sequester approximately a tenth of all carbon emissions (Goudriaan, 1995; Pasher et al., 2014; van Kooten et al., 2019). Despite such an important service to the earth system, forests are facing an increased threat from human-driven deforestation and degradation (Wise et al., 2009). Forests around the world are cleared to create space for agriculture and urban settlement among other land-use types. These activities exacerbate the climate change crisis as large amounts of carbon temporarily stored in vegetation are released back into the atmosphere (Houghton et al., 2012; Rokityanskiy et al., 2007). The United Nations Framework Convention on Climate Change (UNFCCC) introduced the Reduced Emission from Deforestation and Degradation Plus (REDD+) as a measure to reduce continuing deforestation (Phelps et al., 2010). REDD+ requires countries to establish measurement, reporting and verification (MRV) systems to report any changes in carbon stocks (Mitchell et al., 2017). In addition to the reporting requirements under REDD+, countries that reduce the degradation of their forestry resources are financially rewarded through carbon credits (Blom et al., 2010). As such, knowledge on the amount of carbon stored in forests is crucial for monitoring forests and subsequently developing climate change mitigation and adaptation policies.

Monitoring changes in forest carbon stocks can be accomplished through traditional routine surveys of permanent plots established in a forest. Although this approach is accurate, it is costly and time-consuming (Henry et al., 2011; Mitchell et al., 2017; Nhamo, 2011). Moreover, observations are limited to a few established permanent plots and thus the results obtained are spatially limited (Dube et al., 2016). Carbon stock estimation through the use of satellite imagery has the capacity to augment and overcome the limitations of ground surveys. Remote sensing reduces the high financial, time and human resource costs owing to its large spatial coverage at limited cost (Gizachew & Duguma, 2016). Remote sensing provides an opportunity to assess an area over large temporal scales hence making it possible to assess trends in carbon stocks (Mareya et al., 2018; Mitchell et al., 2017). Numerous remote sensing instruments that include active sensors and passive sensors such as RADARSAT and Landsat Thematic Mapper (TM), respectively, have been utilised independently in estimating forest carbon stocks in several biomes. Optical remote sensors such as Landsat are highly sensitive to leaf biomass, whereas Radio Detection and Ranging (RADAR) sensors particularly L-band can penetrate tree canopies and sense variation in stem biomass (Naidoo et al., 2015; Sinha et al., 2015). However, none of these sensors is expected to provide infallible estimates of forest carbon stocks. For example, optical imagery is known to saturate in high biomass stands, while RADAR data interpretation is affected by speckles and shadows (Sinha et al., 2015). To this end, an integration of these sensors can potentially overcome their respective limitations and improve forest carbon estimation (Gizachew & Duguma, 2016).

ALOS PALSAR (Advanced Land Observing Satellite Phased Array type L-band Synthetic Aperture RADAR) is an active sensor that emits radio signals towards objects and measures the signal that bounces back to the sensor (Cornforth et al., 2013; Morel et al., 2011). Landsat 7 Enhanced Thematic Mapper (ETM+), on the other hand, is a passive sensor that records the spectral properties of objects based on the sun's electromagnetic radiation (Basuki et al., 2013; Dube & Mutanga, 2015). Landsat imagery has been proven to be sensitive to variations in vegetation structural parameters that include forest carbon stocks (Goetz & Dubayah, 2011). However, this sensor like any other optical sensor is easily affected by clouds and saturates in areas of high biomass (Baccini et al., 2008; Gibbs et al., 2007). The saturation problem is mainly a result of its inability to penetrate complex overlapping canopies in highly foliated landscapes. RADAR sensors on the other hand are not affected by clouds and have the ability to penetrate vegetation canopies and sense stem biomass (Anaya et al., 2009; Gibbs et al., 2007).

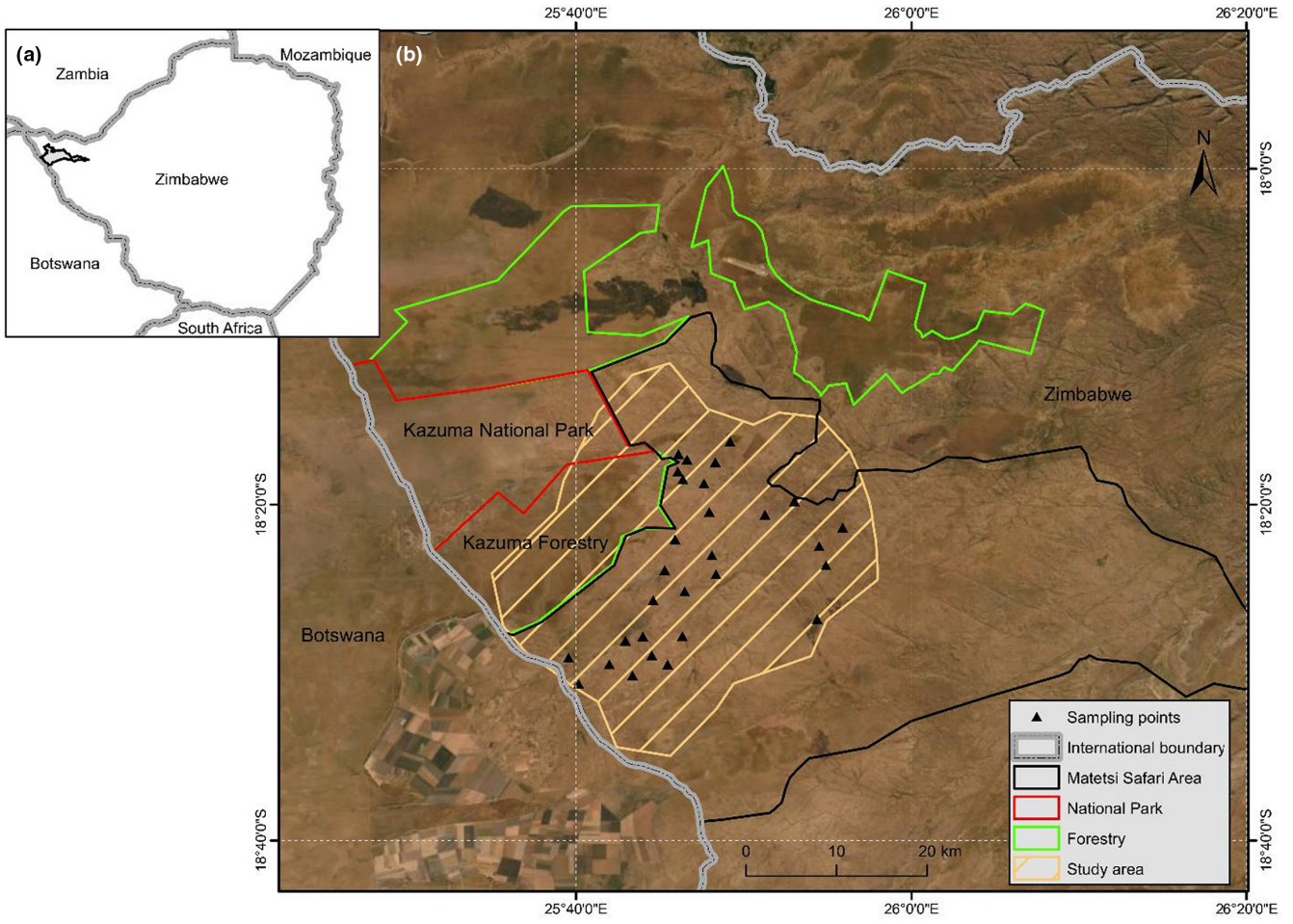

FIGURE 1 (a) The location of Matetsi Safari Area in Zimbabwe and (b) the spatial distribution of sample plots overlaid on RGB Worldview imagery acquired on 15 October 2019.

TABLE 1 Tree allometric equations used to estimate AGB

Species	Allometric equation	Reference
Colophospermum mopane	$AGB = \exp\left(-2.55 + 0.895\ln(D^2H)\right)$	Colgan et al. (2014)
Combretum apiculatum	$AGB = \exp\left(-2.75 + 0.941\ln(D^2H)\right)$	Colgan et al. (2014)
Other species	$AGB = \exp\left(-2.597 + 0.929\ln(D^2H)\right)$	Colgan et al. (2014)

Note: AGB is above-ground biomass, D is basal diameter, H is tree height.

Consequently, a synergy of these two sensors has the potential to improve forest carbon stock estimation.

To date, studies integrating optical and RADAR imagery for improved biomass mapping have focused on tropical monsoon, tropical rain, moist deciduous and temperate forests (Ho Tong Minh et al., 2018; Lehmann et al., 2012; Morel et al., 2012; Sinha et al., 2016; Zhao et al., 2016). To the best of our knowledge, no study has integrated optical and RADAR imagery for forest carbon modelling in mopane-dominated dry savannah forest of Southern Africa. The few studies that have been conducted in these ecosystems mainly use optical sensors to model forest biomass or carbon (Dube et al., 2016; Gara et al., 2017). Dry savannah forests of Southern Africa are characterised by different vegetation structures compared to tropical monsoon, tropical rain, moist deciduous and temperate forests where radar data have been intensively used. The fundamental difference is with regard to tree density and subsequently biophysical parameters such as leaf area index (LAI) which are key proxies of biomass as an estimate from remote sensing platforms (Crowther et al., 2015). Tropical monsoon and temperate forests are typically denser, with multiple layers of vegetation across the canopy vertical profile. savannah dry forests on the other hand are patchy, often a single layer and with no understory (Charles-Dominique et al., 2015). In this regard, there is an inherent need to investigate the integration of multi-sensors in the estimation of carbon stocks in mopane-dominated savannah dry forests.

This study aims at estimating forest carbon stocks through the integration of optical and RADAR data sets. Specifically, the study seeks to (i) examine the utility of Landsat 7 ETM+ in estimating

forest carbon stocks, (ii) assess the utility of ALOS PALSAR in estimating forest carbon stocks and (iii) integrate Landsat 7 ETM+ and ALOS PALSAR data in mapping forest carbon stocks.

2 | MATERIALS AND METHODS

2.1 | Study area

The present study is based on field data which were collected in part of the Matetsi safari area in Zimbabwe and measures ~39,511 ha (Figure 1). Matetsi safari area is located in the north-eastern part of Zimbabwe between 31°48′–31°55′E and 18°22′–18°27′S. The safari area receives a mean annual precipitation of 600 mm with the rain season spanning from November to April (Childes & Walker, 1987). The vegetation type in Matetsi is predominantly savannah woodland and bushland with some areas occupied by large patches of grassland vegetation (Crosmary et al., 2015). The mopane woodland vegetation in Matetsi is dominated by *Colophospermum mopane* and *Combretum apiculatum* (Ndaimani et al., 2014). The area is dominated by regosols and lithosols soils (Muposhi et al., 2016).

2.2 | Field data

Field data on tree structural variables were collected in April–May 2010. Thirty sampling points were randomly generated in the woodland vegetation class using the vegetation map provided by Zimbabwe Parks & Wildlife Management Authority. A hand-held Global Positioning System (GPS) *Garmin GPSmap 60CSx* (with an error of ±5 m) was used to navigate to sampling locations. At each sampling location, a square plot of 900 m^2, that is 30×30 m was established. Within each sampling plot, all standing trees with a diameter at breast height (DBH) greater than 10 cm and height above 3 m had their structural attributes measured. DBH was measured at a height of 1.3 m above-ground surface using a diameter tape while tree height was determined using a clinometer for each tree. Further details on field measurements are in Gara, Murwira, and Ndaimani (2016a).

Above-ground biomass for each tree was estimated using an appropriate allometric equation presented in Table 1. The estimation of field AGB was accomplished using two types of allometric equations: (i) species-specific equation for the dominant species and (ii) generalised equation for less-dominant species. The plot AGB was subsequently determined as the sum biomass of all trees within each sampling plot. Cognizant of the fact that between 45% and 55% of AGB is carbon, we multiplied AGB with a conversion ratio of 0.47 according to the IPCC guidelines to obtain forest carbon stocks for each plot (IPCC, 2003).

2.3 | Landsat 7 ETM+ pre-processing

Geometrically corrected Landsat 7 ETM+ imagery acquired closet to the date when field data were collected was downloaded from USGS (https://earthexplorer.usgs.gov). The Landsat data set contained strips of no data and gap filling was performed using a mask layer acquired from USGS to populate the empty data strips. In order to reduce the effect of the atmosphere attenuation on measured radiance and obtain top of the atmosphere (TOA) radiance, we performed atmospheric correction on the Landsat 7 ETM+ imagery using the dark object subtraction algorithm in QGIS (Musungu & Mkhize, 2019). Although there exist several other remote sensing products from sensors such as SPOT 5, in this study, we used Landsat 7 ETM+ because it is freely available and the results can be compared with future Landsat missions such as the Landsat 9 launched on 27 September 2021.

2.4 | Vegetation indices

After image pre-processing, vegetation indices (Normalised Difference Vegetation Index (NDVI) (Tucker, 1979) and Simple Ratio (SR) (Jordan, 1969)) presented in Equations 1 and 2 were computed.

$$\mathrm{NDVI} = \frac{\mathrm{NIR} - R}{\mathrm{NIR} + R} \quad (1)$$

$$\mathrm{SR} = \frac{\mathrm{NIR}}{R} \quad (2)$$

where NIR and R stand for near-infrared and red reflectance respectively.

These indices were selected because they generated higher correlations with forest carbon stocks in related studies performed in a similar ecosystem (Dube & Mutanga, 2015; Gara, Murwira, & Ndaimani, 2016a). A suite of other indices such as the soil-adjusted indices were examined and they did not generate better results.

2.5 | ALOS PALSAR pre-processing

RADAR polarisation images (HH and HV, Table 2) were acquired from Japan Aerospace Exploration Agency (JAXA) (https://www.eorc.jaxa.jp/ALOS/en/palsar_fnf/data/index.htm Accessed on 20 January 2020). Speckle filtering, terrain and geometric correction of

TABLE 2 Data sets used in this study

Data set	Tile	Spatial resolution	Acquisition
Landsat 7 ETM+ Level 1C	Path 173 Row 073	30	13 May 2010
ALOS PALSAR	S18E025	25	12 May 2010
ASTER DEM	S19E025	30	Temporal extent of 1 March 2000–30 November 2013

the ALOS PALSAR scene were performed in order to improve the quality of the images before analysis (Flores De Santiago et al., 2013). Speckle filtering was performed to remove speckles and noise present in the images. A geometric correction was done to change the slant distance recorded by the SAR sensor to ground distance. This procedure was performed to correct off-nadir signals acquired by the SAR instruments (Sumantyo & Amini, 2008). Terrain correction, on the other hand, was performed using Advanced Spaceborne Thermal Emission and Reflection Radiometer (ASTER) digital elevation model (DEM) using the topographic correction SAGA Tool in QGIS (Conrad et al., 2015). The radar images acquired in BEAM-DIMAP format were converted from reflectance to backscatter values (which correlates with forest biophysical parameters) using the following formula:

$$\sigma = 10^{*}\log_{10}\left(\mathrm{DN}^{2}\right) + \mathrm{CF}, \tag{3}$$

where DN is the digital number (reflectance values), and CF is the calibration factor of −83 (Shimada et al., 2009).

2.6 | ALOS PALSAR vegetation indices

One of the main objectives of the present study was to integrate ALOS PALSAR and Landsat 7 ETM+ for the purpose of estimating forest carbon stocks. HH, HV radar polarizations and radar vegetation indices were used as input variables in the estimation of forest carbon stocks. The two indices, that is Normalised Backscatter Vegetation Index (Equation 4) (Wagner et al., 1999) and the Radar Vegetation Index (Equation 5) (Li & Wang, 2018), were computed from HH and HV radar polarizations. The NBVI also known as the Radar Forest Degradation Index (RFDI) takes advantage of the high sensitivity of HV polarisation to tree biomass and the moderate sensitivity of HH polarisation to generate an index that ranges from 0 to 1 with patches of high biomass assuming values closer to 1.

$$\mathrm{NBVI} = \frac{\sigma\mathrm{HH} - \sigma\mathrm{HV}}{\sigma\mathrm{HH} + \sigma\mathrm{HV}}, \tag{4}$$

$$\mathrm{RVI} = \frac{4\,\sigma\mathrm{HV}}{\sigma\mathrm{HH} + \sigma\mathrm{HV}}, \tag{5}$$

where σHV and σHH measures of backscattering intensities as measured by the HH and HV polarisation.

2.7 | Harmonising the satellite data sets

ALOS PALSAR and Landsat 7 ETM+ images have different spatial resolutions (25 and 30 m, respectively, Table 2). Therefore, in order to harmonise the two data sets, spatial resampling was performed. This procedure was done to match the spatial resolution of the satellite data sets together with the size of the sampling plot used for field data collection. The images were resampled to 10 m using the nearest neighbour resampling method. After resampling the images, we extracted the image values for each plot as a mean of nine (9) pixels (3 × 3 pixels) to match the size of the sampling plot based on which biomass was estimated.

2.8 | Correlation analysis between predictor variables and forest carbon stocks

Before modelling forest carbon stocks using artificial neural networks, Pearson's correlation coefficient (*r*) was used to examine the strength of the relationship between all predictor variables from ALOS PALSAR and Landsat 7 ETM+ (Gara, Murwira, & Ndaimani, 2016a; Morel et al., 2011) and forest carbon stocks. Correlation analysis explored the strength of the relationship between forest carbon stocks and satellite data from the two sensors. To limit model complexity and achieve model parsimony, we selected Landsat 7 ETM+ spectral bands that generated higher correlations with forest carbon stocks.

2.9 | Modelling forest carbon stocks using artificial neural networks

Artificial neural networks (ANN) are machine-learning algorithms within artificial intelligence machine-learning techniques (Bermejo et al., 2019), whose function imitates the operation of neural networks of a human brain (Ayensa et al., 2017). The structure of a typical ANN is primarily comprised of an input layer, a hidden layer and an output layer. Predictor variables from Landsat 7 ETM+ and ALOS PALSAR data sets were fed into the artificial neural network through the input layer. The hidden layer performed the machine-learning computations and predicted the dependent variable (forest carbon stocks) in the output layer. In this study, three experimental designs were conducted to examine the performance of ALOS PALSAR and Landsat 7 ETM+ imagery.

(i) ALOS PALSAR experiment: FCS ~ HH + HV + NBVI + RVI
(ii) Landsat 7 ETM+ experiment: FCS ~ NDVI + SR + G + NI
(iii) Sensor integration experiment: FCS ~ HH + HV + NBVI + RVI + NDVI + SR + G + NIR (FCS: forest carbon stocks).

Validation of all models for each experimental design was done in two steps. Firstly, we used a leave-one-out-cross-validation (LOOCV) technique (Varma & Simon, 2006) to validate the stability of each model against measured forest carbon stocks. Secondly, we bootstrapped the ANN models with 1000 iterations and a decay threshold value of 0.1 in order to generate numerous models that would facilitate the comparison of root mean square errors (RMSE) generated from the model replicates of each experimental design. The performance of each model was assessed using the coefficient of determination (R^2) and normalised RMSE (nRMSE) between the predicted and measured forest carbon stocks (Thumaty et al., 2016). We also compared the mean nRMSE of the 1000 model iterations for each data set using one-way ANOVA. Subsequently, we

performed a pairwise comparison using *Tukey's* HSD post hoc test. Artificial neural network models were calibrated using the NNET library (Ripley et al., 2016) in *R* statistical software using the 'caret' package (Kuhn, 2012).

3 | RESULTS

The HV polarisation generated the highest correlation ($r = 0.5$) with forest carbon stocks compared to any other ALOS PALSAR variables including the HH polarisation ($r = 0.33$) (Figure 2). The two spectral indices developed from ALOS PALSAR polarisations demonstrated moderate relationships with forest carbon stocks (NBVI = 0.38 and RVI = 0.39). The Landsat 7 ETM+ NIR band and NDVI generated high correlations ($r = 0.39$ and 0.4, respectively) to forest carbon stocks compared to the green band and simple ratio vegetation index ($r = 0.35$ and 0.36, respectively). The NIR and green bands of Landsat 7 ETM+ bands were selected as they exhibited a significant relationship to forest carbon stocks compared to other spectral bands (result not shown).

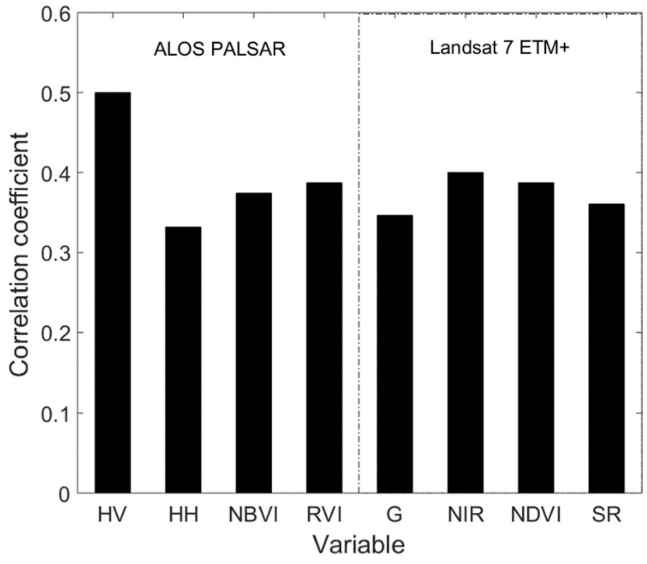

FIGURE 2 Strength of relationship between variables and forest carbon stocks. All correlations were statistically significant at $p > 0.05$.

Based on the LOOCV method both the RMSE and nRMSE decreased in the order of ALOS PALSAR > Landsat ETM > Integrated sensors (Figure 3). Sensor integration yielded an R^2 of 0.84 and nRMSE of 0.12 compared to ALOS PALSAR and Landsat 7 ETM+ which generated R^2 of 0.75 and 0.78 together with nRMSE of 0.16 and 0.14, respectively.

The nRMSE generated from the bootstrapped ANN models confirmed the significant decrease in error in the order of ALOS PALSAR > Landsat ETM+ > Integrated sensors (Figure 4). ALOS PALSAR models yielded a mean nRMSE of 0.26, while Landsat 7 ETM+ generate an nRMSE of 0.23. However, when data from the two sensors were integrated into the ANN modelling nRMSE significantly dropped to 0.18. A *Tukey* post hoc test showed that the nRMSE generated by both the ALOS PALSAR and Landsat 7 ETM+ were significantly different from those yielded by the Integrated model (Figure 4).

Figure 5 shows the spatial variation in forest carbon stocks mapped using the best-performing ANN model, that is the integrated model. The spatial distribution of forest carbon stocks is consistent with findings observed during fieldwork, which showed that stands at higher elevations had higher carbon content than low-lying areas because they had less vegetative cover.

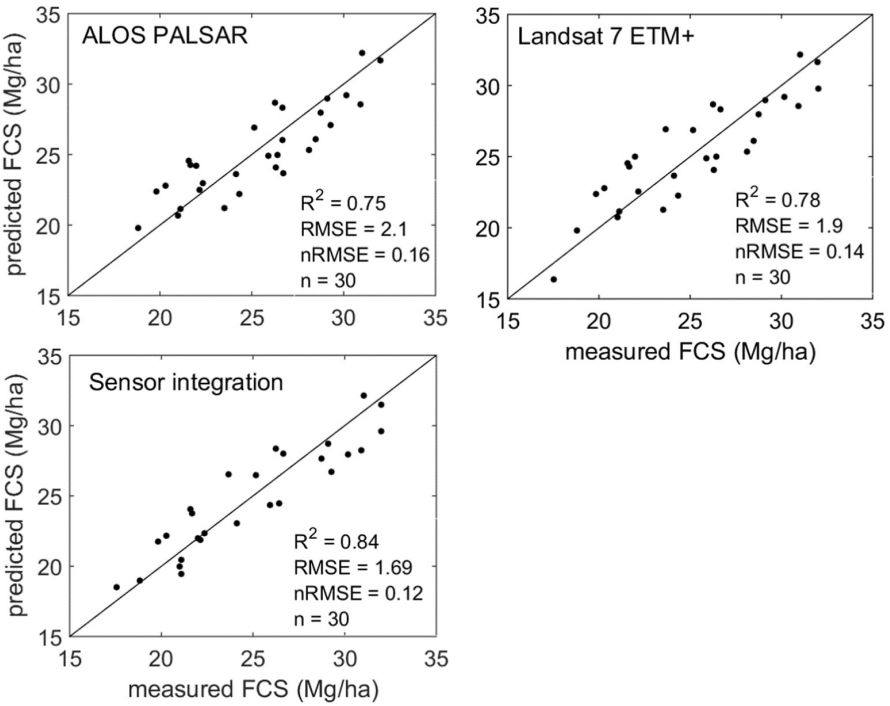

FIGURE 3 Leave-one-out cross-validation of the ANN model for the three data sets.

4 | DISCUSSION

Results presented in this study demonstrate that integrating Landsat 7 ETM+ and ALOS PALSAR improve the estimation accuracy of forest carbon stocks in a dry mopane woodland in comparison to independently modelling forest carbon stocks using data from Landsat 7 ETM+ or ALOS PALSAR. ALOS PALSAR produced an R^2 of 0.75 and nRMSE of 16% and Landsat ETM+ generated an R^2 of 0.78 and nRMSE of 14% based the on leave-one-out cross-validation (Figure 3). However, when the data from the two sensors were integrated the R^2 improved to 0.84 and the nRMSE dropped to 12%. A comparison of the mean nRMSE generated from the 1000 model iterations further confirmed the improvement in the estimation accuracy of the data integration approach (Figure 4). As expected, the mean nRMSE of several model iterations is higher compared to the nRMSE generated from the leave-one-out-cross-validation procedure. These results concur with observations made by Basuki et al. (2013), Chen et al. (2009), Ho Tong Minh et al. (2018) and Shao and Zhang (2016) who observed an improvement in biomass modelling after fusing optical and RADAR imageries. For example, Shao and Zhang (2016) observed an increase in estimation accuracy (from 18.68% to 14.17%) after integrating Landsat 8 OLI and RADARSAT-2 to estimate above-ground biomass in Mongolia, China. Our results demonstrate that ALOS PALSAR and Landsat 7 ETM+ complement each other and their integration is beneficial for forest carbon modelling.

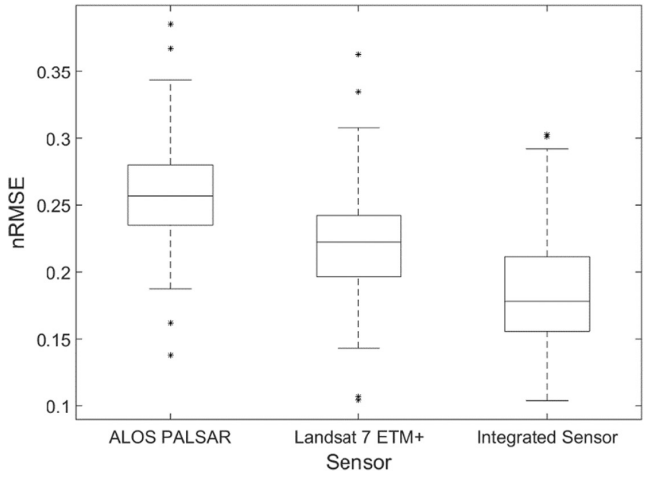

FIGURE 4 Distribution of the nRMSE based on the bootstrapped ANN model for each dataset

Landsat 7 ETM+ provides information in the optical spectral domain (400–2500 nm), which reflects variation in canopy biochemical and biomass content. For example, reflectance in the NIR spectral bands is sensitive to foliage biomass or leaf area index (Soudani et al., 2006; Xavier & Vettorazzi, 2004), while the visible bands respond to variation in chlorophyll pigmentation (Ali et al., 2020; Croft et al., 2013, 2015). This confirms the high correlation observed for the green and NIR Landsat 7 ETM+ bands (Figure 2). ALOS PALSAR on the other hand has the ability to penetrate the canopy and provide information on stem biomass. The single polarised HV generated a higher correlation to forest carbon stocks compared to the HH signal (Figure 2). HH consists mainly of surface canopy scattering while HV reflects volumetric scattering because of its ability to penetrate the canopy and thus corresponds to variation in biomass and forest carbon stocks (Collins et al., 2009; Morel et al., 2011). We report for the first time that ALOS PALSAR indices (NBVI and RVI) generate a moderate correlation with forest carbon stocks in a savannah dry forest. Our study generated a higher R^2 compared to Goh et al. (2014) who obtained an R^2 value of 0.46 and nRMSE of 0.36 after integrating a

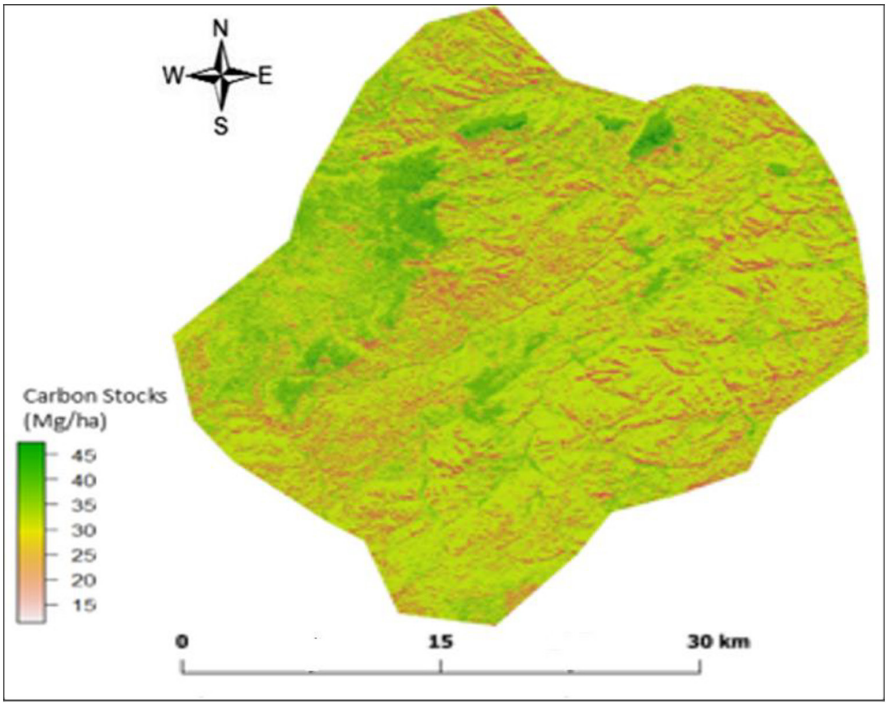

FIGURE 5 Spatial distribution of forest carbon stocks based on the integrated model. Underneath the forest carbon map is a digital elevation model. The Mg/ha represents megagram = 1000 kg

SPOT-5 NIR band with an HV polarisation band from ALOS PALSAR in a study carried out in Singapore. This variation can be attributed to the procedure in which data integration was performed in our study. In their study, Goh et al. (2014) integrated spectral bands alone without using vegetation indices, especially the radar indices which are documented to improve vegetation biophysical retrieval. Moreover, our study used a powerful machine-learning technique ANN, compared to simple parametric linear regression used in several studies (Basuki et al., 2013; Wingate et al., 2018). The utility of ANN concurs with Foody et al. (2003) who modelled forest biomass using ANN based on Landsat TM imagery in Malaysia.

In as much as the models produced in this study had high predictive power, like all modelling processes they are subject to error. The possible source of errors include uncertainties in the allometric equations used especially the generalised species. Errors in a model can also be propagated from atmospheric and geometric processing of the images. However, an error of less than 25% is considered a good estimate and sufficient in vegetation biophysical predictions using remote sensing data (Asner et al., 2015). Our results thus demonstrate high prediction accuracies for all three experimental models. The spatial variation in forest carbon stocks shown in Figure 5 reflects the foraging behaviour of key foraging wildlife species in the park. The park has a sizeable number of African elephants, and they forage in accessible low-lying areas rather than inaccessible high-elevation areas (Gara, Wang, et al., 2016b).

To the best of our knowledge, a single study (Wingate et al., 2018) has to date integrated radar and optical imagery to estimate forest carbon stocks or any other forest structural parameter in the savannah dry forest of Southern Africa. Studies that have examined the utility of radar remote sensing have mainly focused on tropical forests while savannah dry forests of Southern Africa have remained under-reported. The few studies conducted in these ecosystems used Landsat data only and regressed forest carbon stocks to vegetation indices using simple parametric regression (Gara et al., 2015, 2017). In addition to integrating ALOS PALSAR and Landsat ETM+, our study demonstrates the utility of ANN—a parametric machine-learning algorithm to estimate and map forest carbon stocks.

4.1 | Implications for management

The findings presented in this study have a wide range of policy implications related to UNFCCC carbon stock measurement, reporting and verification (Herold & Skutsch, 2011). Our findings validate the use of remote sensing as a tool to supplement in situ measurements of carbon stocks for estimating and monitoring a key forest metric across large landscapes in an understudied forest type. Future management of these fragile ecosystems depends on an understanding of how changes in forest carbon stocks relate to changes in land use and cover as well as to other types of disturbance. The map that was created is crucial for identifying and selecting landscapes with mutually beneficial features in addition to assessing the spatial variability in forest carbon stocks (for biodiversity conservation, habitat extent and fragmentation).

5 | CONCLUSION

In this study, we examined the utility of integrating ALOS PALSAR and Landsat 7 ETM+ in estimating forest carbon stocks in a savannah dry forest. Based on the results obtained from our analysis, we conclude that

(i) Integrating ALOS PALSAR and Landsat 7 ETM+ bands and vegetation indices improves the estimation accuracy of forest carbon stocks in mopane dry forests compared to when they are used as independent data sets.
(ii) An integrated RADAR and Landsat 7 ETM data set can be successfully used to map variability in forest carbon stocks in a savannah dry forest.
(iii) The spatial variation in forest carbon stocks generally reflects the foraging behaviour of key foraging wildlife species, that is African elephants in the study site.

However, further research should be conducted in the other biomes using the recently launched Sentinels SAR and Landsat imagery to ascertain the validity of the results obtained in this study.

ACKNOWLEDGEMENTS

The authors extend their gratitude to Zimbabwe Parks and Wildlife Authority (ZimParks) for allowing us access to the Matetsi Safari Area.

FUNDING INFORMATION

This work received no funding.

CONFLICT OF INTEREST

The authors reported no potential conflict of interest.

DATA AVAILABILITY STATEMENT

The data that support the findings of this study are available from the corresponding author upon reasonable request.

ORCID

Tawanda W. Gara https://orcid.org/0000-0001-8134-4849
Kudzai S. Mpakairi https://orcid.org/0000-0002-1929-1464

REFERENCES

Ali, A. M., Darvishzadeh, R., Skidmore, A., Gara, T. W., O'Connor, B., Roeoesli, C., Heurich, M., & Paganini, M. (2020). Comparing methods for mapping canopy chlorophyll content in a mixed mountain forest using Sentinel-2 data. *International Journal of Applied Earth Observation and Geoinformation*, *87*, 102037.

Anaya, J. A., Chuvieco, E., & Palacios-Orueta, A. (2009). Aboveground biomass assessment in Colombia: A remote sensing approach. *Forest Ecology and Management*, *257*, 1237–1246.

Asner, G. P., Martin, R. E., Anderson, C. B., & Knapp, D. E. (2015). Quantifying forest canopy traits: Imaging spectroscopy versus field survey. *Remote Sensing of Environment*, *158*, 15–27.

Ayensa, J., Doweidar, M. H., Sanz-Herrera, J. A., & Doblare, M. (2017). A new reliability-based data-driven approach for noisy experimental data with physical constraints. *Computer Methods in Applied Mechanics and Engineering*, *328*, 752–774.

Baccini, A., Laporte, N., Goetz, S., Sun, M., & Dong, H. (2008). A first map of tropical Africa's above-ground biomass derived from satellite imagery. *Environmental Research Letters*, *3*, 045011.

Basuki, T. M., Skidmore, A. K., Hussin, Y. A., & Van Duren, I. (2013). Estimating tropical forest biomass more accurately by integrating ALOS PALSAR and Landsat-7 ETM+ data. *International Journal of Remote Sensing*, *34*, 4871–4888.

Bermejo, J. F., Fernández, J. F. G., Polo, F. O., & Márquez, A. C. (2019). A review of the use of artificial neural networks models for energy and reliability prediction. A study for the solar PV, hydraulic and wind energy sources. *Applied Sciences*, *9*, 1844.

Blom, B., Sunderland, T., & Murdiyarso, D. (2010). Getting REDD to work locally: Lessons learned from integrated conservation and development projects. *Environmental Science & Policy*, *13*, 164–172.

Charles-Dominique, T., Staver, A. C., Midgley, G. F., & Bond, W. J. (2015). Functional differentiation of biomes in an African savanna/forest mosaic. *South African Journal of Botany*, *101*, 82–90.

Chen, W., Blain, D., Li, J., Keohler, K., Fraser, R., Zhang, Y., Leblanc, S., Olthof, I., Wang, J., & McGovern, M. (2009). Biomass measurements and relationships with Landsat-7/ETM+ and JERS-1/SAR data over Canada's western sub-arctic and low arctic. *International Journal of Remote Sensing*, *30*, 2355–2376.

Childes, S. L., & Walker, B. H. (1987). Ecology and dynamics of the woody vegetation on the Kalahari Sands in Hwange National Park, Zimbabwe. *Vegetatio*, *72*, 111–128.

Colgan, M. S., Swemmer, T., & Asner, G. P. (2014). Structural relationships between form factor, wood density, and biomass in African savanna woodlands. *Trees*, *28*, 91–102.

Collins, J., Hutley, L. B., Williams, R., Boggs, G., Bell, D., & Bartolo, R. (2009). Estimating landscape-scale vegetation carbon stocks using airborne multi-frequency polarimetric synthetic aperture radar (SAR) in the savannahs of North Australia. *International Journal of Remote Sensing*, *30*, 1141–1159.

Conrad, O., Bechtel, B., Bock, M., Dietrich, H., Fischer, E., Gerlitz, L., Wehberg, J., Wichmann, V., & Böhner, J. (2015). System for automated geoscientific analyses (SAGA) v. 2.1. 4. *Geoscientific Model Development*, *8*(7), 1991–2007.

Cornforth, W. A., Fatoyinbo, T. E., Freemantle, T. P., & Pettorelli, N. (2013). Advanced land observing satellite phased array type L-band SAR (ALOS PALSAR) to inform the conservation of mangroves: Sundarbans as a case study. *Remote Sensing*, *5*, 224–237.

Croft, H., Chen, J., Zhang, Y., & Simic, A. (2013). Modelling leaf chlorophyll content in broadleaf and needle leaf canopies from ground, CASI, Landsat TM 5 and MERIS reflectance data. *Remote Sensing of Environment*, *133*, 128–140.

Croft, H., Chen, J. M., Zhang, Y., Simic, A., Noland, T., Nesbitt, N., & Arabian, J. (2015). Evaluating leaf chlorophyll content prediction from multispectral remote sensing data within a physically-based modelling framework. *ISPRS Journal of Photogrammetry and Remote Sensing*, *102*, 85–95.

Crosmary, W. G., Côté, S., & Fritz, H. (2015). Does trophy hunting matter to long-term population trends in African herbivores of different dietary guilds? *Animal Conservation*, *18*, 117–130.

Crowther, T. W., Glick, H. B., Covey, K. R., Bettigole, C., Maynard, D. S., Thomas, S. M., Smith, J. R., Hintler, G., Duguid, M. C., Amatulli, G., Tuanmu, M. N., Jetz, W., Salas, C., Stam, C., Piotto, D., Tavani, R., Green, S., Bruce, G., Williams, S. J., … Bradford, M. A. (2015). Mapping tree density at a global scale. *Nature*, *525*, 201–205.

Dube, T., Gara, W. T., Sibanda, M., Shoko, C., Murwira, A., Ndaimani, H., & Hatendi, C. (2016). Estimating forest standing biomass in savanna woodlands as an indicator of forest productivity using the new generation WorldView-2 sensor. *Geocarto International*, *33*, 1–21.

Dube, T., & Mutanga, O. (2015). Evaluating the utility of the medium-spatial resolution Landsat 8 multispectral sensor in quantifying aboveground biomass in uMgeni catchment, South Africa. *ISPRS Journal of Photogrammetry and Remote Sensing*, *101*, 36–46.

Flores De Santiago, F., Kovacs, J. M., & Lafrance, P. (2013). An object-oriented classification method for mapping mangroves in Guinea, West Africa, using multipolarized ALOS PALSAR L-band data. *International Journal of Remote Sensing*, *34*, 563–586.

Foody, G. M., Boyd, D. S., & Cutler, M. E. J. (2003). Predictive relations of tropical forest biomass from Landsat TM data and their transferability between regions. *Remote Sensing of Environment*, *85*(4), 463–474.

Gara, T. W., Murwira, A., Dube, T., Sibanda, M., Rwasoka, D. T., Ndaimani, H., Chivhenge, E., & Hatendi, C. M. (2017). Estimating forest carbon stocks in tropical dry forests of Zimbabwe: Exploring the performance of high and medium spatial-resolution multispectral sensors. *Southern Forests: A Journal of Forest Science*, *79*, 31–40.

Gara, T. W., Murwira, A., & Ndaimani, H. (2016a). Predicting forest carbon stocks from high resolution satellite data in dry forests of Zimbabwe: Exploring the effect of the red-edge band in forest carbon stocks estimation. *Geocarto International*, *31*, 176–192.

Gara, T. W., Murwira, A., Ndaimani, H., Chivhenge, E., & Hatendi, C. M. (2015). Indigenous forest wood volume estimation in a dry savanna, Zimbabwe: Exploring the performance of high-and-medium spatial resolution multispectral sensors. *Transactions of the Royal Society of South Africa*, *70*, 285–293.

Gara, T. W., Wang, T., Skidmore, A. K., Zengeya, F. M., Ngene, S. M., Murwira, A., & Ndaimani, H. (2016b). Understanding the effect of landscape fragmentation and vegetation productivity on elephant habitat utilization in Amboseli ecosystem, Kenya. *African Journal of Ecology*, *5*, 259–269.

Gibbs, H. K., Brown, S., Niles, J. O., & Foley, J. A. (2007). Monitoring and estimating tropical forest carbon stocks: Making REDD a reality. *Environmental Research Letters*, *2*, 045023.

Gizachew, B., & Duguma, L. A. (2016). Forest carbon monitoring and reporting for REDD+: What future for Africa? *Environmental Management*, *58*, 922–930.

Goetz, S., & Dubayah, R. (2011). Advances in remote sensing technology and implications for measuring and monitoring forest carbon stocks and change. *Carbon Management*, *2*, 231–244.

Goh, J., Miettinen, J., Chia, A. S., Chew, P. T., & Liew, S. C. (2014). Biomass estimation in humid tropical forest using a combination of ALOS PALSAR and SPOT 5 satellite imagery. *Asian Journal of Geoinformatics*, *13*, 1–17.

Goudriaan, J. (1995). Global carbon cycle and carbon sequestration. In *Carbon sequestration in the biosphere* (pp. 3–18). Springer.

Henry, M., Maniatis, D., Gitz, V., Huberman, D., & Valentini, R. (2011). Implementation of REDD+ in sub-Saharan Africa: State of knowledge, challenges and opportunities. *Environment and Development Economics*, *16*, 381–404.

Herold, M., & Skutsch, M. (2011). Monitoring, reporting and verification for national REDD + programmes: Two proposals. *Environmental Research Letters*, *6*, 014002.

Ho Tong Minh, D., Ndikumana, E., Vieilledent, G., McKey, D., & Baghdadi, N. (2018). Potential value of combining ALOS PALSAR and Landsat-derived tree cover data for forest biomass retrieval in Madagascar. *Remote Sensing of Environment*, *213*, 206–214.

Houghton, R. A., House, J., Pongratz, J., Van Der Werf, G., DeFries, R., Hansen, M., Le Quéré, C., & Ramankutty, N. (2012). Carbon emissions from land use and land-cover change. *Biogeosciences*, *9*, 5125–5142.

IPCC. 2003. Good practice guidance for land use, land-use change and forestry. In *National Greenhouse gas Inventories Programme*. (p. 295). IPCC.

Jordan, C. F. (1969). Derivation of leaf-area index from quality of light on the Forest floor. *Ecology*, *50*, 663–666.

Kuhn, M. 2012. *The caret package. R Foundation for Statistical Computing*. https://cran.r-project.org/package=caret

Lehmann, E. A., Caccetta, P. A., Zhou, Z., McNeill, S. J., Wu, X., & Mitchell, A. L. (2012). Joint processing of Landsat and ALOS-PALSAR data for Forest mapping and monitoring. *IEEE Transactions on Geoscience and Remote Sensing*, *50*, 55–67.

Li, J., & Wang, S. (2018). Using SAR-derived vegetation descriptors in a water cloud model to improve soil moisture retrieval. *Remote Sensing*, *10*, 1370.

Mareya, H. T., Tagwireyi, P., Ndaimani, H., Gara, T. W., & Gwenzi, D. (2018). Estimating tree crown area and aboveground biomass in Miombo woodlands from high-resolution RGB-only imagery. *IEEE Journal of Selected Topics in Applied Earth Observations and Remote Sensing*, *11*, 1–8.

Mitchell, A. L., Rosenqvist, A., & Mora, B. (2017). Current remote sensing approaches to monitoring forest degradation in support of countries measurement, reporting and verification (MRV) systems for REDD+. *Carbon Balance and Management*, *12*, 1–22.

Morel, A. C., Fisher, J. B., & Malhi, Y. (2012). Evaluating the potential to monitor aboveground biomass in forest and oil palm in Sabah, Malaysia, for 2000–2008 with Landsat ETM+ and ALOS-PALSAR. *International Journal of Remote Sensing*, *33*, 3614–3639.

Morel, A. C., Saatchi, S. S., Malhi, Y., Berry, N. J., Banin, L., Burslem, D., Nilus, R., & Ong, R. C. (2011). Estimating aboveground biomass in forest and oil palm plantation in Sabah, Malaysian Borneo using ALOS PALSAR data. *Forest Ecology and Management*, *262*, 1786–1798.

Muposhi, V. K., Gandiwa, E., Chemura, A., Bartels, P., Makuza, S. M., & Madiri, T. H. (2016). Habitat heterogeneity variably influences habitat selection by wild herbivores in a semi-arid tropical savanna ecosystem. *PLoS One*, *11*, e0163084.

Musungu, K., & Mkhize, Z. T. (2019). Change detection in the horticultural region of Cape Town using Landsat imagery. In S. Wade (Ed.), *Earth observations and geospatial science in Service of Sustainable Development Goals* (pp. 69–76). Springer.

Naidoo, L., Mathieu, R., Main, R., Kleynhans, W., Wessels, K., Asner, G., & Leblon, B. (2015). Savannah woody structure modelling and mapping using multi-frequency (X-, C-and L-band) synthetic aperture radar data. *ISPRS Journal of Photogrammetry and Remote Sensing*, *105*, 234–250.

Ndaimani, H., Murwira, A., & Kativu, S. (2014). Predicting the spatial distribution of hunted and non-hunted sable antelope (Hippotragus Niger Niger) using remotely sensed woody cover in a southern African savanna. *Geocarto International*, *29*, 198–210.

Nhamo, G. (2011). REDD+ and the global climate policy negotiating regimes: Challenges and opportunities for Africa. *South African Journal of International Affairs*, *18*, 385–406.

Pasher, J., McGovern, M., Khoury, M., & Duffe, J. (2014). Assessing carbon storage and sequestration by Canada's urban forests using high resolution earth observation data. *Urban Forestry & Urban Greening*, *13*, 484–494.

Phelps, J., Guerrero, M. C., Dalabajan, D. A., Young, B., & Webb, E. L. (2010). What makes a 'REDD'country? *Global Environmental Change*, *20*, 322–332.

Ripley, B., W. Venables, and M. B. Ripley. 2016. Package 'nnet'. R package version. *7*:3–12.

Rokityanskiy, D., Benítez, P. C., Kraxner, F., McCallum, I., Obersteiner, M., Rametsteiner, E., & Yamagata, Y. (2007). Geographically explicit global modeling of land-use change, carbon sequestration, and biomass supply. *Technological Forecasting and Social Change*, *74*, 1057–1082.

Shao, Z., & Zhang, L. (2016). Estimating Forest aboveground biomass by combining optical and SAR data: A case study in Genhe, Inner Mongolia, China. *Sensors (Basel, Switzerland)*, *16*, 834.

Shimada, M., Isoguchi, O., Tadono, T., & Isono, K. (2009). PALSAR radiometric and geometric calibration. *IEEE Transactions on Geoscience and Remote Sensing*, *47*, 3915–3932.

Sinha, S., Jeganathan, C., Sharma, L., & Nathawat, M. (2015). A review of radar remote sensing for biomass estimation. *International journal of Environmental Science and Technology*, *12*, 1779–1792.

Sinha, S., Jeganathan, C., Sharma, L. K., Nathawat, M. S., Das, A. K., & Mohan, S. (2016). Developing synergy regression models with space-borne ALOS PALSAR and Landsat TM sensors for retrieving tropical forest biomass. *Journal of Earth System Science*, *125*, 725–735.

Soudani, K., François, C., Le Maire, G., Le Dantec, V., & Dufrêne, E. (2006). Comparative analysis of IKONOS, SPOT, and ETM+ data for leaf area index estimation in temperate coniferous and deciduous forest stands. *Remote Sensing of Environment*, *102*, 161–175.

Sumantyo, J. T. S., & Amini, J. (2008). A model for removal of speckle noise in SAR images (ALOS PALSAR). *Canadian Journal of Remote Sensing*, *34*, 503–515.

Thumaty, K. C., Fararoda, R., Middinti, S., Gopalakrishnan, R., Jha, C., & Dadhwal, V. (2016). Estimation of above ground biomass for central Indian deciduous forests using ALOS PALSAR L-band data. *Journal of the Indian Society of Remote Sensing*, *44*, 31–39.

Tucker, C. J. (1979). Red and photographic infrared linear combinations for monitoring vegetation. *Remote Sensing of Environment*, *8*, 127–150.

van Kooten, G. C., Johnston, C. M., & Mokhtarzadeh, F. (2019). Carbon uptake and forest management under uncertainty: Why natural disturbance matters. *Journal of Forest Economics*, *34*, 159–185.

Varma, S., & Simon, R. (2006). Bias in error estimation when using cross-validation for model selection. *BMC Bioinformatics*, *7*, 91.

Wagner, W., Lemoine, G., Borgeaud, M., & Rott, H. (1999). A study of vegetation cover effects on ERS scatterometer data. *IEEE Transactions on Geoscience and Remote Sensing*, *37*, 938–948.

Wingate, V. R., Phinn, S. R., Kuhn, N., & Scarth, P. (2018). Estimating aboveground woody biomass change in Kalahari woodland: Combining field, radar, and optical data sets. *International Journal of Remote Sensing*, *39*, 577–606.

Wise, M., Calvin, K., Thomson, A., Clarke, L., Bond-Lamberty, B., Sands, R., Smith, S. J., Janetos, A., & Edmonds, J. (2009). Implications of limiting CO_2 concentrations for land use and energy. *Science*, *324*, 1183–1186.

Xavier, A. C., & Vettorazzi, C. A. (2004). Monitoring leaf area index at watershed level through NDVI from Landsat-7/ETM+ data. *Scientia Agricola*, *61*, 243–252.

Zhao, P., Lu, D., Wang, G., Liu, L., Li, D., Zhu, J., & Yu, S. (2016). Forest aboveground biomass estimation in Zhejiang Province using the integration of Landsat TM and ALOS PALSAR data. *International Journal of Applied Earth Observation and Geoinformation*, *53*, 1–15.

How to cite this article: Gara, T. W., Mpakairi, K. S., Nampira, T. C., Oduro Appiah, J., Muumbe, T. P., & Dube, T. (2023). Integrating RADAR and optical imagery improve the modelling of carbon stocks in a mopane-dominated African savannah dry forest. *African Journal of Ecology*, *00*, 1–10. https://doi.org/10.1111/aje.13114